ADVANCED MATERIALS
www.advmat.de

Asymmetric Redox-Polymer Interfaces for Electrochemical Reactive Separations: Synergistic Capture and Conversion of Arsenic

*Kwiyong Kim, Stephen Cotty, Johannes Elbert, Raylin Chen, Chia-Hung Hou, and Xiao Su**

Advanced redox-polymer materials offer a powerful platform for integrating electroseparations and electrocatalysis, especially for water purification and environmental remediation applications. The selective capture and remediation of trivalent arsenic (As(III)) is a central challenge for water purification due to its high toxicity and difficulty to remove at ultra-dilute concentrations. Current methods present low ion selectivity, and require multistep processes to transform arsenic to the less harmful As(V) state. The tandem selective capture and conversion of As(III) to As(V) is achieved using an asymmetric design of two redox-active polymers, poly(vinyl)ferrocene (PVF) and poly-TEMPO-methacrylate (PTMA). During capture, PVF selectively removes As(III) with exceptional uptake (>100 mg As/g adsorbent), and during release, synergistic electrocatalytic oxidation of As(III) to As(V) with >90% efficiency can be achieved by PTMA, a radical-based redox polymer. The system demonstrates >90% removal efficiencies with real wastewater and concentrations of arsenic as low as 10 ppb. By integrating electron-transfer through the judicious design of asymmetric redox-materials, an order-of-magnitude energy efficiency increase can be achieved compared to non-faradaic, carbon-based materials. The study demonstrates for the first time the effectiveness of asymmetric redox-active polymers for integrated reactive separations and electrochemically mediated process intensification for environmental remediation.

Arsenic is one of the pressing environmental hazards in drinking water around the world, with over 200 million inhabitants and 70 countries within the scope of its impact.[1] Naturally occurring mineral deposits of arsenic are ubiquitous around the globe near groundwater sources, with locations such as Bangladesh having over 60% of the population affected by severe arsenic contamination.[1a,2] Arsenic occurs naturally in water as anionic arsenate (As(V)) or arsenite (As(III)), with the latter being acutely toxic and difficult to remove.[3] Commonly employed techniques to remove arsenic are coagulation-flocculation or chemical adsorption, both which require significant chemical input, and extensive pretreatment steps for As(III) to As(V) conversion.[3c] Thus, novel removal technologies that integrate removal and conversion of arsenic are critical for sustainable environmental management.

The development of advanced materials for water purification, selective contaminant removal, and improved energy efficiency is critical to tackling water-energy nexus challenges, including through the design of more effective membranes and field-assisted adsorbents.[4] Electrochemical methods for water treatment such as capacitive deionization (CDI) have garnered increased attention as a desalination technology, and also as a heavy metal removal platform, due to their efficiency and low environmental footprint compared to typical methods.[5] Electrosorption systems benefit from inherent modularity and scalability, which opens the door to point of source remediation systems. Electrochemical conversion of As(III) to As(V) on carbon electrode has been investigated previously for CDI-based arsenic remediation.[5l,6] However, low arsenic selectivity in the presence of competing ions has limited the total uptake capacity of carbon-based CDI,[5c,h–l] as most arsenic contaminated water sources are composed of 10 to 1000-fold excess salts.[7] Thus, the design of molecularly selective functional adsorbents is necessary to address these materials chemistry limitations.

Recent work has shown redox-active/Faradaic materials as an attractive platform for selective water contaminant removal.[8] Redox-active metallopolymers have demonstrated remarkable uptake of anions with significant selectivity, both of organic anions and heavy metal oxyanions.[8b,9] At the same time, asymmetric electrochemical systems have traditionally been proposed in energy-storage applications to enhance capacitance and electrochemical properties.[10] Here, we leverage this electrochemical design for the first time to integrate both the separation and the reactions step electrochemically at functionalized electrodes. We seek to combine two redox-active polymer

Dr. K. Kim, S. Cotty, Dr. J. Elbert, R. Chen, Prof. X. Su
Department of Chemical and Biomolecular Engineering
University of Illinois at Urbana-Champaign
Urbana, IL 61801, USA
E-mail: x2su@illinois.edu
Prof. C.-H. Hou
Graduate Institute of Environmental Engineering
National Taiwan University
Taipei 10617, Taiwan
The ORCID identification number(s) for the author(s) of this article can be found under https://doi.org/10.1002/adma.201906877.

DOI: 10.1002/adma.201906877

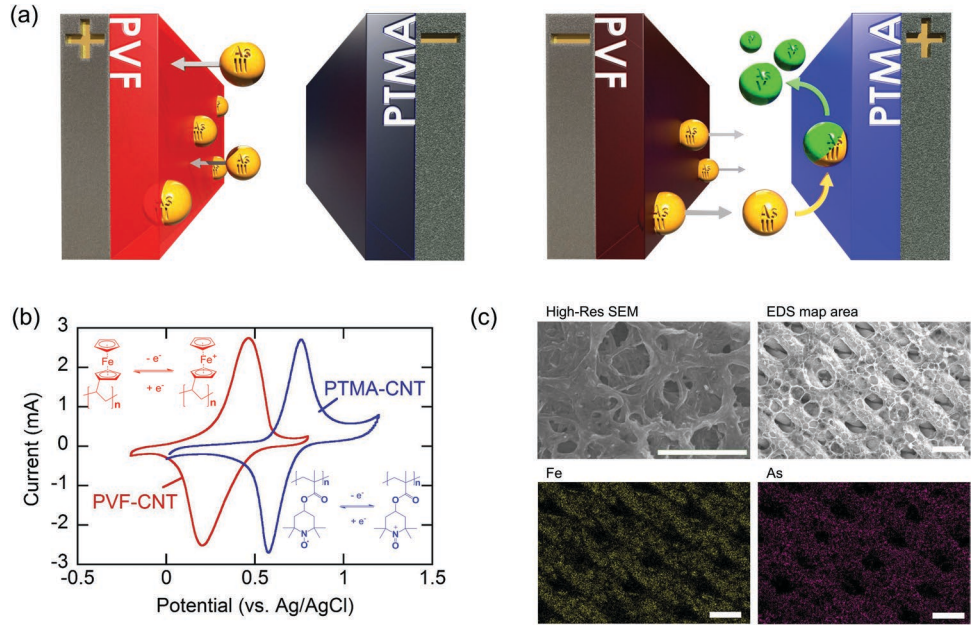

Figure 1. a) Schematic illustrations showing selective separation by PVF-CNT during adsorption and reactive conversion by PTMA-CNT during desorption (left: adsorption, right: desorption). b) A cyclic voltammogram of a fully asymmetric faradaic system with PVF-CNT and PTMA-CNT electrode. c) Scanning electron microscopy (SEM) images of the PVF-CNT electrode after adsorption of arsenic, and EDS mapping of iron on the ferrocene unit of PVF-CNT, and of adsorbed arsenic. Scale bar for High-resolution SEM image is 1 µm, and scale bar for EDS and Fe/As mapping is 50 µm.

electrodes to enable the selective capture of trivalent arsenic, As(III), and devise a process to achieve tandem conversion during release by taking advantage of the intrinsic electron-transfer coupling in asymmetric systems.

Tandem Faradaic systems have been successfully used previously as a medium to minimize side-reactions and increase current efficiency.[8c,11] In this study, an asymmetric redox-active design is proposed, in which a working electrode is functionalized with a poly(vinyl)ferrocene (PVF), and the counter-electrode with poly-TEMPO-methacrylate (PTMA), a polymer containing redox-active nitroxide radical moieties (see **Figure 1**a). Redox-active species have shown great promise in terms of acting as high-charge materials,[8c,12] as well as their electrocatalytic properties for organic pollutant decontamination.[13] Nitroxide radicals, the best-known example being 2,2,6,6-tetramethylpiperidine-*N*-oxyl (TEMPO), show a unique redox behavior. One-electron reduction leads to the hydroxylamine anions, whereas one-electron oxidation generates the oxoammonium cations.[14] The cationic form of TEMPO ($TEMPO^+$) is a strong oxidant and highly catalytic, so it is known to rapidly oxidize primary alcohols, such as 5-hydroxymethylfurfural.[15] PTMA is an easily synthesizable TEMPO-based polymer with a high theoretical capacity (111 mAh g^{-1}) and well known redox behavior.[14a] We took advantage of its fast electron transfer processes and higher oxidation potential, exploring the potential of PTMA-CNT as a heterogeneous catalyst on the counter-electrode, to synergistically promote the tandem remediation of As(III). During adsorption, trivalent arsenic is captured by PVF through selective binding, whereas during desorption, TEMPO-mediated conversion of released As(III) into less harmful As(V) is achieved (Figure 1a). The coupled regeneration with conversion in our asymmetric redox design enables energy integration, thereby allowing an order-of-magnitude efficiency increase compared to non-faradaic, carbon-based arsenic removal. Our findings indicate the importance of tandem materials selection and electrochemical integration for selective remediation systems.

First, poly(vinyl)ferrocene/carbon nanotube composites (PVF-CNT) were prepared by a dip-coating method, with excellent mechanical and electrochemical properties.[16] High-resolution scanning electron microscopy showed that the PVF-CNT electrodes were thin films with uniform and nanoporous features (Figure 1c and Figure S2.2: Supporting Information), and energy-dispersive spectroscopy (EDS) mapping clearly showed the strong percentage of redox-units immobilized (22% Fe). Galvanostatic charge–discharge measurements indicated a specific capacity of PVF-CNT was 82.4 mAh g^{-1} (Figure S1.6, Supporting Information). To highlight the performance of our asymmetric system, we initially confirmed the electrosorption capability of PVF-CNT to adsorb As(III) individually, without the redox-counter, and then explored how the combined reactive separation of the asymmetric system overcomes the limitations of conventional systems and provides a superior performance for electroseparation and electroconversion.

PVF-CNT electrodes were first studied as a heterogeneous electrode for the selective uptake of As(III) using a conductive electrode as a counter (PVF-CNT//Pt configuration). Electrosorption of arsenic was carried out by oxidizing Fc units into Fc^+ and thus enabling the selective binding of trivalent arsenic anions (Figure 1a, left). As a control, pure carbon-nanotube electrodes at +0.8 V, or PVF-CNT electrode at open circuit (OC) did not show any affinity toward arsenic (**Figure 2**a,b), which was also confirmed by X-ray photoelectron spectroscopy (XPS) analysis (Figure S3.2, Supporting Information). When

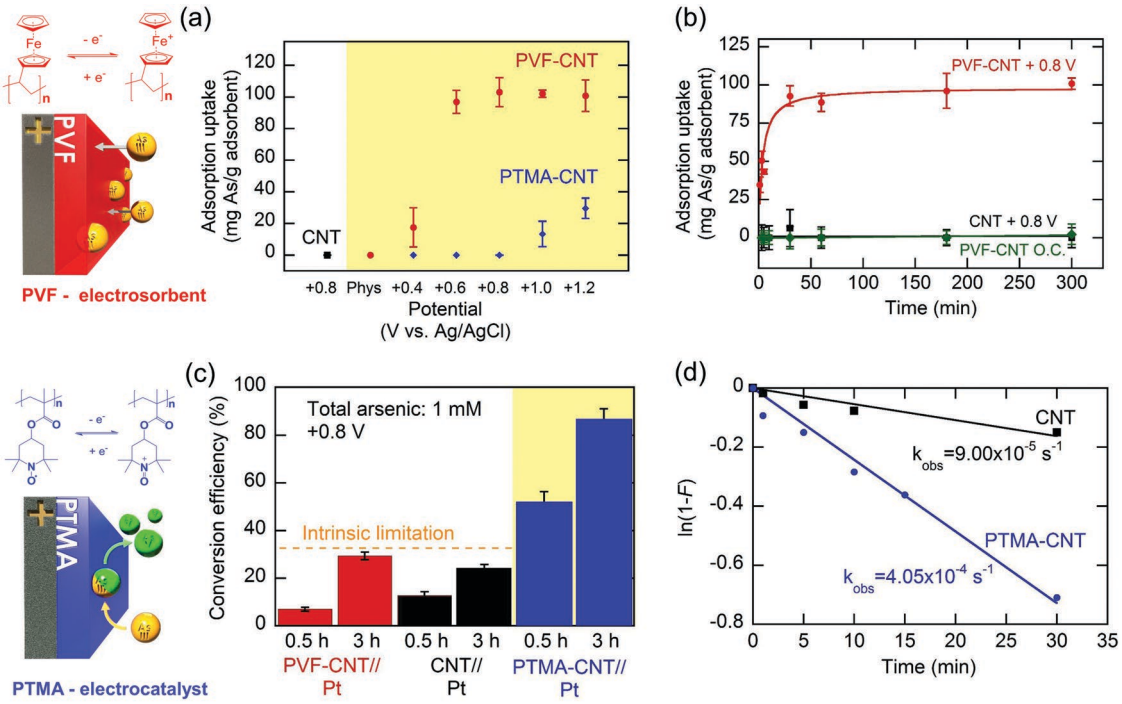

Figure 2. Performance of PVF as an electrosorbent: a) Comparison of arsenic uptake capacity of PVF-CNT, CNT, and PTMA-CNT electrode, in an electrolyte containing 1×10^{-3} M $NaAsO_2$ and 20×10^{-3} M NaCl for 30 min. There was no arsenic uptake on PVF-CNT at open circuit, and much higher uptake capacity for PVF-CNT than CNT is observed at +0.8 V versus Ag/AgCl (counter electrode: Pt). b) Adsorption kinetics of arsenic by PVF-CNT and CNT electrodes at +0.8 V. Performance of PTMA as an electrocatalyst: c) Percentage of oxidized As(V) species after polarization of various working electrodes at +0.8 V in 1×10^{-3} M $NaAsO_2$ and 20×10^{-3} M NaCl. d) Kinetics of the conversion of As(III) to As(V) in 1×10^{-3} M $NaAsO_2$ and 20×10^{-3} M NaCl using CNT or PTMA-CNT as a working electrode polarized at +0.8 V. F denotes the conversion into As(V).

the applied potential onto PVF-CNT was varied, potential higher than +0.4 V led to similarly high uptake of arsenic, reaching 103.1 mg arsenic/g adsorbent after 30 min at +0.8 V. Furthermore, comparable arsenic uptake (78.7 mg arsenic/g adsorbent) was obtained using 1×10^{-3} M pentavalent As(V) as initial feedstock (Figure S4.1, Supporting Information). All these results demonstrated the superior uptake, fast adsorption kinetics, and significant selectivity of PVF-based arsenic removal compared to conventional carbon-based electrosorption or other nanoparticle sorbents reported in literature.[3d,5h–l] Prior studies have shown charge-transfer interactions of As(V) anions toward metallopolymers,[9] with current results indicating the strong counter-ion binding with the trivalent form.

X-ray photoelectron spectroscopy analysis highlighted that the application of positive potential oxidized over 64.8% of the Fc sites, and higher potentials resulted in even more oxidized Fc^+ (Figure S3.3 and Table S3.2, Supporting Information). After electrosorption at +0.8 V (vs Ag/AgCl) for 3 h in 1×10^{-3} M $NaAsO_2$ and 20×10^{-3} M NaCl, the PVF-CNT surface was saturated with adsorbed arsenic, as seen through EDS mapping (Figure 1c). Strong interaction of arsenic-ferrocenium binding was further indicated by an atomic ratio analysis of the PVF-CNT surface after electrosorption with As(III) as the minority ion (1×10^{-3} M AsO_2^- and 20×10^{-3} M Cl^-); almost equal stoichiometric ratio of iron to arsenic (1.07:1.00) (Table S3.1, Supporting Information). With the arsenic to chloride ratio being >2.45, PVF-CNT shows strongly selective binding of As(III) to Fc unit, leading to a separation factor of 49:1 over competing ions (Cl^-). The selectivity mechanism can be attributed to the strong charge-transfer mechanisms between ferrocenium and the bound counter-ions, in accordance with previous observations of cyclopentadienyl interactions.[8b]

In order to design an asymmetric configuration that can enable tandem electrosorption and electrocatalysis, the counter-electrode must promote redox-transformation of the arsenic (III) oxyanion at an appropriate voltage window while suppressing any re-adsorption of the oxyanion. A 2,2,6,6-tetramethylpiperidinyl-*N*-oxyl containing polymer, poly(4-methacryloyloxy-2,2,6,6-tetramethylpiperidin-1-oxyl) (PTMA) was synthesized and blended with CNT by a similar dip-coating method (PTMA-CNT).[16] Similarly with PVF-CNT, PTMA-CNT exhibited homogeneous and nanoporous morphology (Figure S2.3, Supporting Information), with a specific capacitance of 75.6 mAh g^{-1} estimated from galvanostatic measurements (Figure S1.6, Supporting Information). Electron paramagnetic resonance (EPR) measurements indicated a radical yield of 72.5% for the PTMA polymer (Figure S1.5, Supporting Information), which is in the comparable range to literature values.[17]

The cyclic voltammogram (CV) of a balanced dual-functionalized PVF-CNT//PTMA-CNT is shown in Figure 1b. The position of potentials in the individual CVs indicated that their redox processes are shifted to be suitable counter-electrodes, which contributed to the minimization of re-adsorption of arsenic; charging of PVF-CNT at +0.8 V led to remarkable adsorption, whereas the same potential led to no adsorption onto PTMA-CNT (Figure 2a). More importantly, PTMA behaved

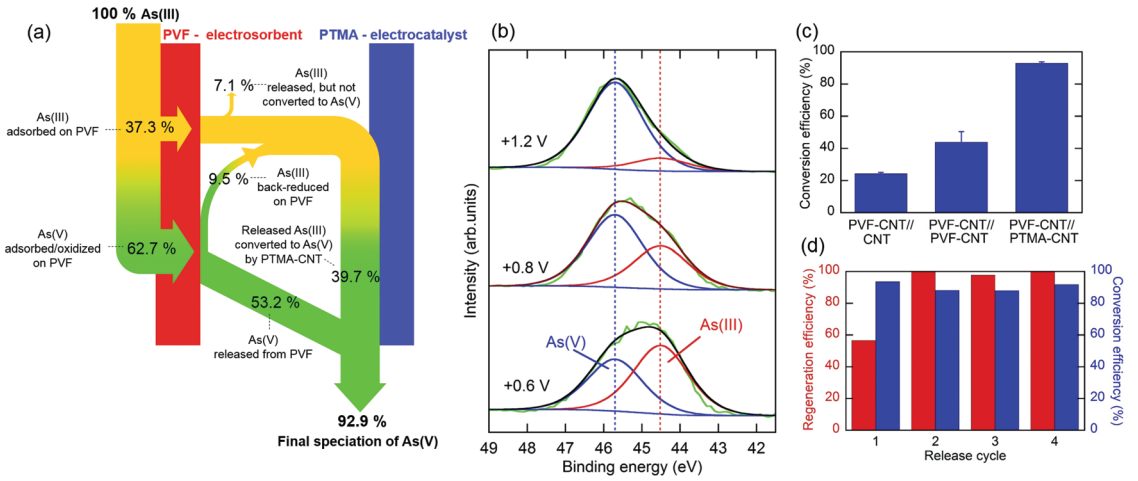

Figure 3. a) A flow diagram showing the speciation of arsenic in asymmetric PVF-CNT (electroadsorbent)//PTMA-CNT (electrocatalyst) configuration. b) High resolution As3d spectra of the PVF-CNT electrode after adsorption at +0.6, +0.8, and +1.2 V. c) Conversion efficiency of various configurations after one cycle of adsorption and desorption (adsorption: +0.8 V on PVF-CNT, desorption: +0.8 V on counter electrode). d) Recyclability of the asymmetric PVF-CNT//PTMA-CNT system over a number of cycles (adsorption: +0.8 V on PVF-CNT, desorption: +0.8 V on PTMA-CNT), as given by regeneration efficiency (red) and conversion efficiency (blue).

as an excellent electrocatalyst for arsenic conversion into As(V), exhibiting exceptional conversion efficiency (Figure 2c), current efficiency (Figure S4.3, Supporting Information) and also a five-times higher conversion rate than unfunctionalized carbon at +0.8 V, with k_{obs} (observed rate constant) being 4.05×10^{-4} and 9.00×10^{-5} s^{-1} for PTMA-CNT and CNT, respectively by using a first order kinetic fit–as seen in Figure 2d.[18] The TEMPO-mediated conversion of As(III) to As(V) is hypothesized to involve the oxoammonium cations ($TEMPO^+$), which is a strong oxidant.[19] The high current efficiency of 90.4% (Figure S4.3, Supporting Information) for arsenic conversion proves that almost all of $TEMPO^+$ produced via anodic charging participate in mediated conversion of As(III), and is hypothesized to follow a catalytic mechanism that cycles between $TEMPO^+$ and the neutral form of TEMPO radical.[14a,19] The two-electron oxidation of As(III) to As(V) can either occur cooperatively, by oxidation enabled by two adjacent TEMPO units on the PTMA-chain, or possibly, As(III) oxidation may proceed in a stepwise/sequential manner via the formation of a reported metastable intermediate As(IV).[20] A detailed mechanistic study is planned in the future to elucidate and confirm the exact pathways for TEMPO-mediated As(III) conversion to As(V). The enhanced conversion by PTMA inspired us to utilize PTMA-CNT as an asymmetric counter electrode coupled with PVF-CNT, and operate a process at a working potential of +0.8 V on PVF-CNT (adsorption), and then sequentially apply the oxidation potential to PTMA-CNT (desorption) to achieve tandem separation and conversion within the same electrochemical unit.

A careful speciation of arsenic was carried out between the liquid and solid-phase by spectroscopy and spectrophotometric assay. In accordance with the thermodynamic equilibrium of arsenic species in aqueous phase (see Pourbaix diagram in Figure S7.1 in the Supporting Information), the oxidation of surface-bound As(III) to As(V) on PVF-CNT during electrosorption was corroborated by the XPS surface analysis; 62.7% of surface-adsorbed As(III) was shown to be converted to As(V) at +0.8 V (**Figure 3**a), with stronger peak intensity for oxidized form As(V) at higher potential (Figure 3b and Table S3.3: Supporting Information), according to surface As speciation analysis.[21] In the desorption stage, PMTA-CNT was charged at +0.8 V, leading to a PVF-CNT polarization between −0.4 and −0.2 V as shown in Figure S5.5 (Supporting Information), within a region where back-reduction of As(V) to As(III) could occur (see Pourbaix diagram in Figure S7.1 in the Supporting Information). The quantitative back-reduction into As(III) at the surface of PVF-CNT after regeneration was tracked by XPS (Figure S3.4 and Table S3.3, Supporting Information). It was observed that the speciation of residual, surface-adsorbed As(V) was decreased to 53.2% after regeneration. Based on this speciation analysis (Figure 3a), 46.8% (37.3% + 9.5%) of released arsenic was estimated to leave PVF-CNT without being converted into As(V). The arsenic speciation analysis highlights the need for implementing a reactive oxidation at the opposite electrode, thus overcoming thermodynamic and kinetic limits of using solely a PVF-CNT adsorbent.

With the asymmetric PVF-CNT//PTMA-CNT system, after regeneration of PVF-CNT electrode by charging PTMA-CNT at +0.8 V, most of the released As(III) (including those from back-reduction) was almost completely oxidized by TEMPO-mediated catalysis, thereby accomplishing a final conversion of 92.9% into the less harmful, pentavalent state of As(V) (Figure 3a,c). This provides strong evidence that catalytic conversion by PTMA was coupled with the regeneration of PVF-CNT in a simultaneous manner to assist in arsenic remediation. As a control, the use of a CNT or PVF-CNT counter led to a much lower final conversion of arsenic (Figure 3c). Even worse, PVF-CNT//CNT or symmetric PVF-CNT//PVF-CNT also showed poor regeneration (<40%), either due to a lower current efficiency of the CNT counter (Figure S5.5, Supporting Information), or re-adsorption of arsenic anions in the case of the symmetric PVF-CNT counter. By cycling PVF-CNT//PTMA-CNT system, the conversion efficiency was retained at close to or

higher than 90% over a number of cycles (Figure 3d), demonstrating the stability of PTMA-CNT as a redox counter and as an electrocatalyst. At the same time, the regeneration efficiency was maintained at about 100% starting at cycle 2 (Figure 3d). The incomplete initial regeneration in cycle 1 was probably due to the loss from coagulation or irreversible binding onto some Fc sites, as noted also from XPS (Table S3.1, Supporting Information).[22] Even so, the steady working capacity of PVF-CNT (>54 mg As/g adsorbent) was preserved during multiple cycles. Furthermore, there was no noticeable increase or decrease in solution pH upon repeated adsorption and desorption for 4 cycles (Figure S6.2, Supporting Information) except for the change due to As(III) conversion ($H_2O + H_2AsO_3^- \rightarrow HAsO_4^{2-} + 3H^+ + 2e^-$), showing that dual-functionalized asymmetric redox system can effectively suppress parasitic side-reactions.[8c] Finally, continuous cycling of the asymmetric system in the arsenic-containing electrolyte for 60 cycles indicated the reversible, stable nature of our redox-active electrodes (Figure S5.6, Supporting Information).

We investigated the performance of our asymmetric systems using real secondary effluent wastewater collected from Urbana-Champaign Sanitary District spiked with 100 ppb As(III). It was observed that over 90% removal efficiency was achieved within 2 h of electrosorption, satisfying the 10 ppb WHO guideline with an operational cell voltage significantly lower than the water electrolysis window (**Figure 4**a).[23] Following the results obtained at analytical batch scale, the system was scaled up to a flow-by electrochemical cell with a 16-times larger electrode area (Figure 4b). The PVF and PTMA flow-by electrodes were prepared using a drop-and-smear method, producing a uniform electrode coating (see Section S1.4 in the Supporting Information). The chronoamperotmetric adsorption (+2 V) and desorption (–2 V) under continuous flow (1.5 mL min^{-1}) of 1×10^{-3} M arsenic resulted in the total cumulative uptake of 51.9 mg arsenic/g adsorbent, and the release of 81.9% of the adsorbed arsenic (Figure 4b), corresponding well with batch results. Our flow-based studies establish a proof-of-concept, and show that further engineering optimization can yield even higher performance metrics.

Finally, an evaluation of energy integration and consumption for the combined reactive separation was carried out to highlight the intrinsic performance advantages of using redox-active materials (see Section S8 in the Supporting Information for calculation details). By relying on the intrinsic energy storage and recovery properties of redox-active materials, we can achieve remarkable energy-efficiency enhancement as well as molecular integration of our electrochemical processes. First, control experiments investigating the electrosorption based on porous carbon, a traditional non-Faradaic CDI material, was estimated to use 5.83 kWh mol As^{-1} for the separation of arsenic, due to low selectivity of the carbon adsorbents (**Figure 5**a,c). On the other hand, experimental runs applying a redox-active anode (PVF-CNT) enabled a high separation factor during electrosorption, lowering the amount of energy input in the adsorption process to 0.76 kWh mol As^{-1} (Figure 5b,c). The optimization of the fully asymmetric redox systems (PVF-CNT//PTMA-CNT) resulted in an even lower energy input by minimizing the applied voltage window through tuning of the redox-potentials (Figure 1b). Chronopotentiometry at 0.1 mA cm^{-2} exhibited a working electrode potential of 0.52 V, and counter-electrode

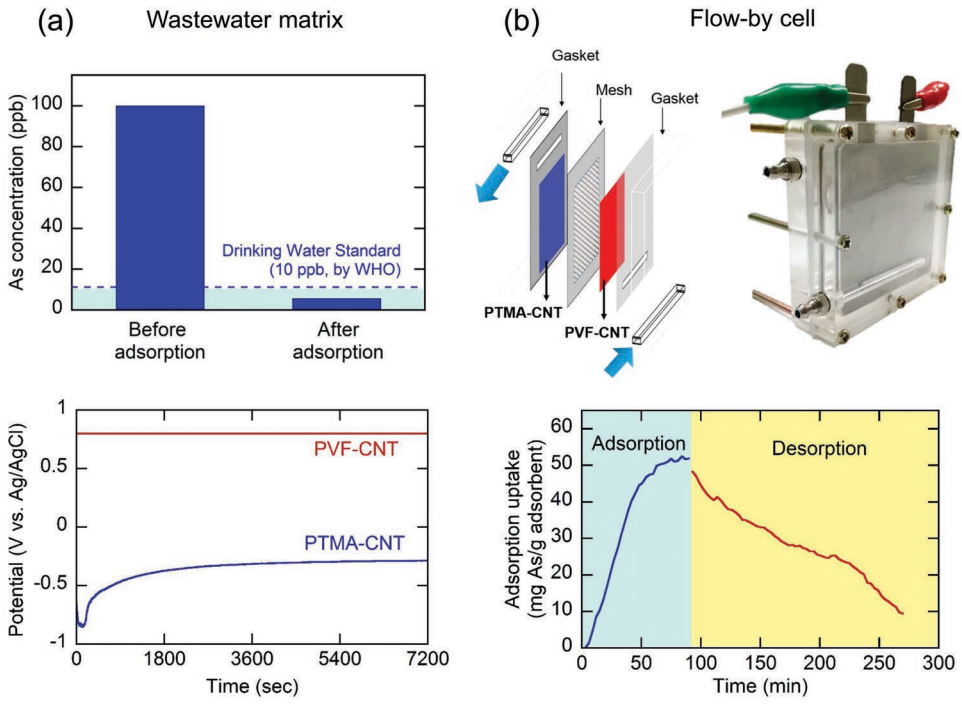

Figure 4. a) Wastewater matrix: Removal of arsenic under municipal secondary wastewater effluent solution (obtained from Urbana-Champaign Sanitary District) spiked with As(III) at 100 ppb. +0.8 V was applied for 2 h; Simultaneous tracking of anode (PVF-CNT) and cathode (PTMA-CNT) potentials during charging of asymmetric electrochemical systems at 0.8 V (PVF-CNT). b) A flow-by cell: A schematic design of the flow-by cell system used in this study; Adsorption and desorption of arsenic during charging and discharging (within a 2 V cell window).

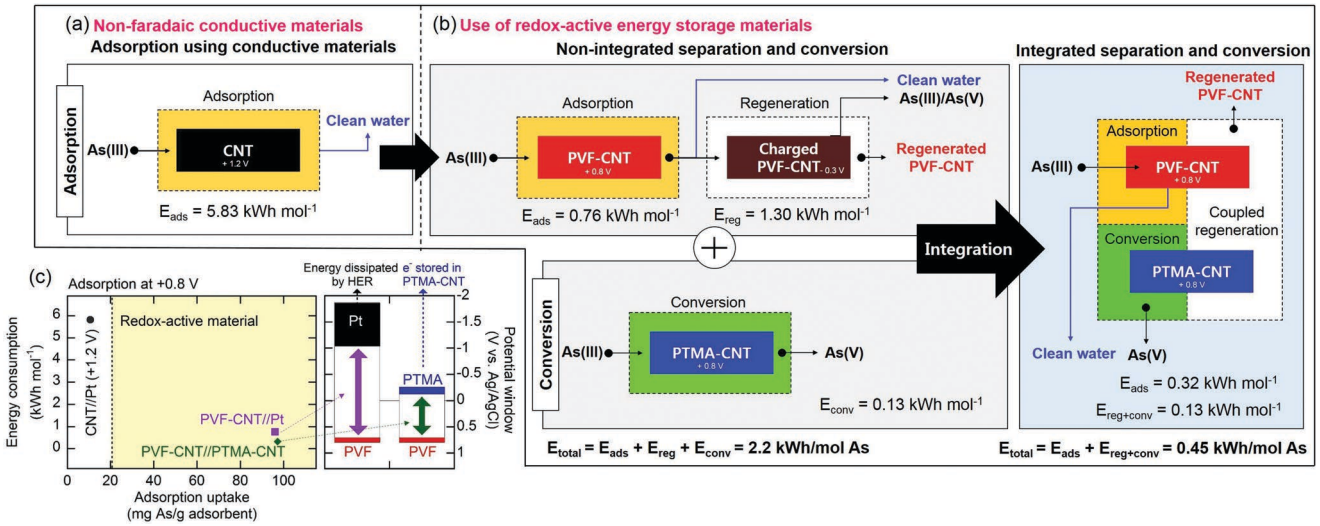

Figure 5. The integration of energy input using redox-electrochemistry. a) Energy consumption during adsorption by non-faradaic conductive material (CNT) at +1.2 V. b) Energy consumption of nonintegrated adsorption by PVF-CNT and conversion by PTMA-CNT. The rightmost figure shows the fully integrated system with asymmetric redox-active polymers, and a comparison of the energy input for separation and conversion of arsenic in each unit process. c) A summary of energy consumption during adsorption by CNT, PVF-CNT with a conductive counter electrode, and PVF-CNT with a redox-active counter electrode and their corresponding electrochemical potential window of each electrode.

potential of −0.38 V (Figure S5.1, Supporting Information) using the fully asymmetric system, which lowers the overall voltage requirement (0.9 V), contrary to the conductive, non-redox counter electrodes (Figure S5.2, Supporting Information). When the system was operated under constant voltage, the two different configurations (PVF-CNT//Pt and PVF-CNT//PTMA-CNT) exhibited the same trend in current density (Figure S5.3, Supporting Information) and arsenic uptake (Figure S4.2, Supporting Information), but a much lower overpotential was required for a redox PTMA-CNT counter compared to a conductive counter (Figure 5c and Figure S5.4: Supporting Information). As a result, the fully asymmetric PVF-CNT//PTMA-CNT only consumed 0.32 kWh mol As^{-1} for the separation process (Figure 5b,c). When a conductive counter was used, hydrogen evolution became a major cathodic reaction with a large overpotential, not only dissipating energy but also leading to harmful change in water chemistry which impacts separation efficiency.[8c] By leveraging PTMA-CNT on the counter-electrode, we can efficiently store electrons through the TEMPO redox electrochemistry, which during discharge can be not only used as an electron donor for PVF-CNT regeneration, but also participate in the coupled conversion of As(III) to As(V).

The coupled electron-transfer process and associated energy integration is key to enabling more efficient electrocatalysis and minimizing overall energy consumption (Figure S8.1, Supporting Information). To illustrate, in a regular electrochemical process in which there is no asymmetric integration, the utilization of PVF-CNT and PTMA-CNT in a non-integrated sequential process requires 2.2 kWh mol As^{-1} for separation, regeneration, and conversion in total (Figure 5b). On the other hand, a fully asymmetric redox-system allows an energy integration approach, in which the recovered energy could be directly applied to simultaneous, coupled conversion process, thereby utilizing only 0.45 kWh mol As^{-1} for both selective separation and reactive conversion (Figure 5b). Furthermore, a parametrization of working potential and current density indicated that even more energy-efficient adsorption is possible by varying the potential (Figure S8.2, Supporting Information) or current density (Figure S8.3, Supporting Information)—thus showing that further optimization on cell parameters could push the overall efficiency even higher. Thus, our energy analysis proved an order-of-magnitude efficiency increase of the redox-active, asymmetric system compared to traditional non-faradaic, carbon-based or a sequential process, by closely leveraging electrochemical approaches to create next-generation, energy-integrated water purification devices.

In sum, we have shown that a dual-redox asymmetric configuration, PVF-CNT//PTMA-CNT, allows the integration of separation and transformation of harmful trivalent As(III) within a single unit step. PVF-CNT is shown to be effective for selective capture of trivalent arsenic in the presence of excess competing ions, with fast kinetics and a high adsorption capacity. When a TEMPO-based redox counter was utilized (PTMA-CNT), the asymmetric configuration coupled the selective separation by PVF-CNT in tandem with the simultaneous catalytic conversion of As(III) into the less harmful As(V). Selective removal allows for the purification of a contaminated arsenic stream to clean water, and the release allows for the remediation of the toxic waste product. The performance was further benchmarked using real wastewater samples spiked with ultra-diluted concentration of arsenic, and comparable uptake and release was demonstrated using a flow-by cell (PVF-CNT//PMTA-CNT), showing remarkable separation factors and the practical applicability of this system.

Our proposed redox-polymer system enables integrated reactive separations without the need for chemical regenerants or additives, and based solely on redox-electrochemistry, with an order-of-magnitude improvement in energy efficiency. Our

work illustrates the importance of judicious selection of redox-materials in the asymmetric system, to enable tandem synergistic processes. Going forward, we expect further development of molecularly designed redox materials with superior stability performance, to enable next-generation devices for water purification and environmental remediation. We envision our work to lay the ground for asymmetric redox-systems to be deployed as process intensification platforms for future applications in chemical processing, sustainable environmental separations, and even coupled energy storage devices.

Supporting Information

Supporting Information is available from the Wiley Online Library or from the author.

Acknowledgements

K.K. and S.C. contributed equally to this work. The authors acknowledge the support of the University of Illinois, Urbana-Champaign for startup funding, and the support of the National Science Foundation under Grant #1931941. SEM and XPS were carried out in the Frederick Seitz Materials Research Laboratory Central Research Facilities, University of Illinois. Major funding for the Bruker EMXPlus was provided by National Science Foundation Award 1726244 (2017) to the School of Chemical Sciences EPR lab at the University of Illinois, Urbana-Champaign. The authors thank Loi Chen and Kristina Roth for their aid in the experiments with the flow-by electrochemical cell, and Dr. Toby Woods for assistance with the EPR measurements. The authors also thank Haley Vapnik for her help with the GPC measurements.

Conflict of Interest

The authors declare no conflict of interest.

Keywords

arsenic, electrochemical separation, reactive conversion, redox-active polymers

Received: October 19, 2019
Revised: November 16, 2019
Published online: December 3, 2019

[1] a) M. L. Polizzotto, B. D. Kocar, S. G. Benner, M. Sampson, S. Fendorf, *Nature* **2008**, *454*, 505; b) Y. Lee, I.-H. Um, J. Yoon, *Environ. Sci. Technol.* **2003**, *37*, 5750; c) Y. Q. Qin, F. Peng, Y. G. Hu, *Green Chem.* **2019**, *21*, 2286.

[2] S. A. Ahmad, M. H. Khan, M. Haque, *Risk Manage. Healthcare Policy* **2018**, *11*, 251.

[3] a) F. C. Knowles, A. A. Benson, *Trends Biochem. Sci.* **1983**, *8*, 178; b) K. Coddington, *Toxicol. Environ. Chem.* **1986**, *11*, 281; c) N. R. Nicomel, K. Leus, K. Folens, P. Van der Voort, G. Du Laing, *Int. J. Environ. Res. Public Health* **2016**, *13*, 62; d) B. A. Manning, S. E. Fendorf, B. Bostick, D. L. Suarez, *Environ. Sci. Technol.* **2002**, *36*, 976.

[4] a) Y. Han, Z. Xu, C. Gao, *Adv. Funct. Mater.* **2013**, *23*, 3693; b) H. Qiu, M. Xue, C. Shen, Z. Zhang, W. Guo, *Adv. Mater.* **2019**, *31*, e1803772; c) D. Pakulski, W. Czepa, S. D. Buffa, A. Ciesielski, P. Samorì, *Adv. Funct. Mater.* **2019**, 1902394; d) H. Wang, X. Mi, Y. Li, S. Zhan, *Adv. Mater.* **2019**, 1806843.

[5] a) J. Lee, S. Kim, C. Kim, J. Yoon, *Energy Environ. Sci.* **2014**, *7*, 3683; b) J. Lee, S. Kim, J. Yoon, *ACS Omega* **2017**, *2*, 1653; c) M. E. Suss, S. Porada, X. Sun, P. M. Biesheuvel, J. Yoon, V. Presser, *Energy Environ. Sci.* **2015**, *8*, 2296; d) G. H. Chen, *Sep. Purif. Technol.* **2004**, *38*, 11; e) T. Kim, C. A. Gorski, B. E. Logan, *Environ. Sci. Technol. Lett.* **2017**, *4*, 444; f) Z. Ge, X. Chen, X. Huang, Z. J. Ren, *Environ. Sci.: Water Res. Technol.* **2018**, *4*, 33; g) Z. Huang, L. Lu, Z. Cai, Z. J. Ren, *J. Hazard. Mater.* **2016**, *302*, 323; h) L. Liu, W. Tan, S. L. Suib, G. Qiu, L. Zheng, S. Su, *Chem. Eng. J.* **2019**, *375*, 122051; i) C. S. Fan, S. C. Tseng, K. C. Li, C. H. Hou, *J. Hazard. Mater.* **2016**, *312*, 208; j) C. S. Fan, S. Y. H. Liou, C. H. Hou, *Chemosphere* **2017**, *184*, 924; k) M. Dai, M. Zhang, L. Xia, Y. Li, Y. Liu, S. Song, *ACS Sustainable Chem. Eng.* **2017**, *5*, 6532; l) M. Dai, L. Xia, S. Song, C. Peng, J. R. Rangel-Mendez, R. Cruz-Gaona, *Appl. Surf. Sci.* **2018**, *434*, 816.

[6] Z. Song, S. Garg, J. Ma, T. D. Waite, *Environ. Sci. Technol.* **2019**, *53*, 9715.

[7] a) N. R. Council, *Arsenic in Drinking Water: 2001 Update*, The National Academies Press, Washington, DC **2001**; b) World Health Organization, Vol. WHO/SDE/WSH/03.04/75, **2003**.

[8] a) X. Su, T. A. Hatton, *Adv. Colloid Interface Sci.* **2017**, *244*, 6; b) X. Su, H. J. Kulik, T. F. Jamison, T. A. Hatton, *Adv. Funct. Mater.* **2016**, *26*, 3394; c) X. Su, K.-J. Tan, J. Elbert, C. Rüttiger, M. Gallei, T. F. Jamison, T. A. Hatton, *Energy Environ. Sci.* **2017**, *10*, 1272.

[9] X. Su, A. Kushima, C. Halliday, J. Zhou, J. Li, T. A. Hatton, *Nat. Commun.* **2018**, *9*, 4701.

[10] a) Z. Li, Z. Xu, H. Wang, J. Ding, B. Zahiri, C. M. B. Holt, X. Tan, D. Mitlin, *Energy Environ. Sci.* **2014**, *7*, 1708; b) M. R. Lukatskaya, B. Dunn, Y. Gogotsi, *Nat. Commun.* **2016**, *7*, 12647; c) Y. Shao, M. F. El-Kady, J. Sun, Y. Li, Q. Zhang, M. Zhu, H. Wang, B. Dunn, R. B. Kaner, *Chem. Rev.* **2018**, *118*, 9233.

[11] S. Kim, G. Piao, D. S. Han, H. K. Shon, H. Park, *Energy Environ. Sci.* **2018**, *11*, 344.

[12] J. Lee, P. Srimuk, S. Fleischmann, X. Su, T. A. Hatton, V. Presser, *Prog. Mater. Sci.* **2019**, *101*, 46.

[13] X. Su, L. Bromberg, K. J. Tan, T. F. Jamison, L. P. Padhye, T. A. Hatton, *Environ. Sci. Technol. Lett.* **2017**, *4*, 161.

[14] a) K.-A. Hansen, J. P. Blinco, *Polym. Chem.* **2018**, *9*, 1479; b) L. Bugnon, C. J. H. Morton, P. Novak, J. Vetter, P. Nesvadba, *Chem. Mater.* **2007**, *19*, 2910.

[15] a) Z. G. Zhou, L. X. Liu, *Curr. Org. Chem.* **2014**, *18*, 459; b) D. J. Chadderdon, L. P. Wu, Z. A. McGraw, M. Panthani, W. Li, *ChemElectroChem* **2019**, *6*, 3387.

[16] a) X. Du, Z. Chen, Z. Li, H. Hao, Q. Zeng, C. Dong, B. Yang, *Adv. Energy Mater.* **2014**, *4*, 1400135; b) X. Su, J. Hübner, M. J. Kauke, L. Dalbosco, J. Thomas, C. C. Gonzalez, E. Zhu, M. Franzreb, T. F. Jamison, T. A. Hatton, *Chem. Mater.* **2017**, *29*, 5702.

[17] a) Y. Zhang, A. Park, A. Cintora, S. R. McMillan, N. J. Harmon, A. Moehle, M. E. Flatte, G. D. Fuchs, C. K. Ober, *J. Mater. Chem. C* **2018**, *6*, 111; b) A. Cintora, H. Takano, M. Khurana, A. Chandra, T. Hayakawa, C. K. Ober, *Polym. Chem.* **2019**, *10*, 5094.

[18] L. Bromberg, X. Su, T. A. Hatton, *ACS Appl. Mater. Interfaces* **2013**, *5*, 5468.

[19] J. C. Siu, G. S. Sauer, A. Saha, R. L. Macey, N. Fu, T. Chauvire, K. M. Lancaster, S. Lin, *J. Am. Chem. Soc.* **2018**, *140*, 12511.

[20] a) Z. Wang, R. T. Bush, L. A. Sullivan, C. Chen, J. Liu, *Environ. Sci. Technol.* **2014**, *48*, 3978; b) M. Sun, G. Zhang, Y. Qin, M. Cao, Y. Liu, J. Li, J. Qu, H. Liu, *Environ. Sci. Technol.* **2015**, *49*, 9289; c) M. A. Hasnat, M. M. Hasan, N. Tanjila, M. M. Alam, M. M. Rahman, *Electrochim. Acta* **2017**, *225*, 105; d) K. Mitsudo, T. Shiraga, D. Kagen, D. Shi, J. Y. Becker, H. Tanaka, *Tetrahedron* **2009**, *65*, 8384; e) M. M. Alam, M. A. Rashed, M. M. Rahman,

Mohammed M. Rahman, Y. Nagao, M. A. Hasnat, *RSC Adv.* **2018**, *8*, 8071; f) A. Wiebe, T. Gieshoff, S. Mohle, E. Rodrigo, M. Zirbes, S. R. Waldvogel, *Angew. Chem., Int. Ed. Engl.* **2018**, *57*, 5594.

[21] a) S. Liu, N. Qin, J. Song, Y. Zhang, W. Cai, H. Zhang, G. Wang, H. Zhao, *Talanta* **2016**, *160*, 225; b) X. Han, J. Song, Y. L. Li, S. Y. Jia, W. H. Wang, F. G. Huang, S. H. Wu, *Chemosphere* **2016**, *147*, 337; c) C. H. Liu, Y. H. Chuang, T. Y. Chen, Y. Tian, H. Li, M. K. Wang, W. Zhang, *Environ. Sci. Technol.* **2015**, *49*, 7726; d) W. Yan, M. A. Ramos, B. E. Koel, W. X. Zhang, *Chem. Commun. (Cambridge, UK)* **2010**, *46*, 6995; e) T. Das, C. Mahata, C. K. Maiti, G. K. Dalapati, C. K. Chia, D. Z. Chi, S. Y. Chiam, H. L. Seng, C. C. Tan, H. K. Hui, G. Sutradhar, P. K. Bose, *J. Electrochem. Soc.* **2011**, *159*, G15.

[22] W. Wan, T. J. Pepping, T. Banerji, S. Chaudhari, D. E. Giammar, *Water Res.* **2011**, *45*, 384.

[23] a) L. Chen, X. Dong, F. Wang, Y. Wang, Y. Xia, *Chem. Commun. (Cambridge, UK)* **2016**, *52*, 3147; b) L. Lu, W. Vakki, J. A. Aguiar, C. Xiao, K. Hurst, M. Fairchild, X. Chen, F. Yang, J. Gu, Z. J. Ren, *Energy Environ. Sci.* **2019**, *12*, 1088.